Thymoquinone Triggers Inactivation of the Stress Response Pathway Sensor *CHEK1* and Contributes to Apoptosis in Colorectal Cancer Cells

Hala Gali-Muhtasib,[1] Doerthe Kuester,[2] Christian Mawrin,[3,10] Khuloud Bajbouj,[2] Antje Diestel,[2] Matthias Ocker,[7] Caroline Habold,[1,8] Charlotte Foltzer-Jourdainne,[9] Peter Schoenfeld,[4] Brigitte Peters,[5] Mona Diab-Assaf,[2] Ulf Pommrich,[2] Wafica Itani,[2] Hans Lippert,[6] Albert Roessner,[2] and Regine Schneider-Stock[2]

[1]Department of Biology, American University of Beirut, Beirut, Lebanon; Departments of [2]Pathology, [3]Neuropathology, [4]Biochemistry, [5]Biometrics, and [6]General Surgery of the Otto-von-Guericke University, Magdeburg, Germany; [7]Department of Medicine 1, University Hospital Erlangen, Erlangen, Germany; [8]CEPE-CNRS and [9]INSERM U682, Strasbourg, France; and [10]Department of Neuropathology, Friedrich-Schiller University Jena, Jena, Germany

Abstract

There are few reports describing the role of p53-dependent gene repression in apoptotic cell death. To identify such apoptosis-associated p53 target genes, we used the pro-oxidant plant-derived drug thymoquinone and compared p53+/+ and p53−/− colon cancer cells HCT116. The p53 wild-type (wt) status correlated with more pronounced DNA damage and higher apoptosis after thymoquinone treatment. A significant up-regulation of the survival gene *CHEK1* was observed in p53−/− cells in response to thymoquinone due to the lack of transcriptional repression of p53. In p53−/− cells, transfection with p53-wt vector and CHEK1 small interfering RNA treatment decreased CHEK1 mRNA and protein levels and restored apoptosis to the levels of the p53+/+ cells. p53−/− cells transplanted to nude mice treated with thymoquinone up-regulated CHEK1 expression and did not undergo apoptosis unlike p53+/+ cells. Immunofluorescence analysis revealed that the apoptosis resistance in p53−/− cells after thymoquinone treatment might be conveyed by shuttling of CHEK1 into the nucleus. We confirmed the *in vivo* existence of this CHEK1/p53 link in human colorectal cancer, showing that tumors lacking p53 had higher levels of CHEK1, which was accompanied by poorer apoptosis. CHEK1 overexpression was correlated with advanced tumor stages ($P = 0.03$), proximal tumor localization ($P = 0.02$), and worse prognosis (1.9-fold risk, univariate Cox regression; Kaplan-Meier, $P = 0.04$). We suggest that the inhibition of the stress response sensor CHEK1 might contribute to the antineoplastic activity of specific DNA-damaging drugs. [Cancer Res 2008;68(14):5609–18]

Introduction

p53 was shown to play a critical role in the induction of growth arrest and apoptosis in response to DNA damage by chemotherapeutic agents (1, 2). These multiple functions of p53 are important for tumor suppression, and loss of p53 enhances the risk of developing malignancies (3). p53 triggers cell cycle arrest and apoptosis through transactivation of specific target genes, such as $p21^{WAF1}$, *GADD45*, *Bax*, or *PUMA* (3, 4). Transcriptional activation is mediated by p53 binding to consensus sequences in regulatory regions (5, 6). Recent attempts to identify p53 target genes on a large scale using microarray technology revealed that many p53-responsive genes are repressed rather than activated, and that gene repression by p53 is closely linked to its ability to induce apoptosis (7). Transcriptional repression mechanisms are very complex and are poorly understood (8–10). p53 was shown to down-regulate the DNA damage sensor CHEK1 at the transcriptional level via direct DNA binding (7, 11). This serine/threonine kinase is the major cell cycle checkpoint mediator that is activated upon DNA damage, especially double strand breaks, through the upstream kinases ATH/ATR (12, 13). CHEK1 responds to DNA damage by initiating cell cycle arrest, thus providing time for the cell to repair the damage and to evade apoptosis before resuming cell cycle. Studies have reported that CHEK1 inhibition enhances the cytotoxicity of DNA-damaging agents (14–17). CHEK1 expression constitutes a defense mechanism to circumvent the toxicity of DNA-damaging agents.

Recently, we have shown that the functionality of p53 has a significant effect on cancer cell sensitivity to thymoquinone, an extract of the black seed *Nigella sativa* oil (18, 19). Thymoquinone as a short-chain ubiquinone derivative potentially acts as a pro-oxidant (20). We found that thymoquinone induces cell cycle arrest and apoptosis in HCT116 human colon cancer cells in a p53-dependent manner (18). As it is unclear whether p53-mediated transactivation or transrepression contributes to p53-dependent apoptosis, we used thymoquinone as a tool for oxidative stress induction to identify downstream targets of p53 and to understand their role in p53-induced apoptosis. By comparing the gene expression profiles of HCT116 p53+/+ with p53−/− cells after thymoquinone treatment, *in vitro* and in xenografts, we show that the sensitivity of these cells to thymoquinone-induced apoptosis is due to transcriptional repression of CHEK1 by p53 in p53+/+ HCT116 cells. This is the first report of a CHEK1/p53 link and its prognostic significance in human colorectal cancer tissues.

Materials and Methods

Reagents and drugs. Thymoquinone (>99% pure) was purchased from Fisher Scientific GmbH; Prolong Antifade and propidium iodide were from Molecular Probes. RNase was obtained from Sigma Chemical Co. RPMI 1640, fetal bovine serum, and penicillin-streptomycin were from Life Technologies.

Note: Supplementary data for this article are available at Cancer Research Online (http://cancerres.aacrjournals.org/).

Requests for reprints: Regine Schneider-Stock, Department of Pathology, Otto-von-Guericke University of Magdeburg, Leipziger Strasse 44, 39120 Magdeburg, Germany. Phone: 49-391-6715060; Fax: 49-391-6717839; E-mail: Regine.Schneider-Stock@med.ovgu.de.

doi:10.1158/0008-5472.CAN-08-0884

Preparation of mitochondria. Mitochondria from rat liver were prepared as described previously (21). Details are in the supplement.

Measurement of reactive oxygen species levels. Generation of superoxide ($O_2^{\cdot-}$) by mitochondria was measured as oxidation of Amplex red (Molecular Probes) to resorufin. In the presence of horseradish peroxidase, Amplex red reacts with H_2O_2 to resorufin; mitochondrial protein (0.2 mg) was incubated at 25°C in 1 mL buffer supplemented with 5 μmol/L Amplex red plus horseradish peroxidase (2 units/mL) to detect H_2O_2 and, for quantitative conversion of $O_2^{\cdot-}$ into H_2O_2, with Cu, Zn-dismutase (2 units/mL). Changes in fluorescence were monitored by a Perkin-Elmer LS-50B fluorescence spectrometer (excitation at 560 nm, emission at 590 nm). Fluorescence intensity was calibrated with H_2O_2.

Aconitase activity. Oxidative stress was measured by inactivation of the mitochondrial enzyme aconitase. Enzymatic activity was measured by the formation of NADPH at 340 nm (22). Mitochondrial protein (0.4 mg) was preincubated for 15 min at 37°C in buffer supplemented with thymoquinone. Thereafter, 5 mmol/L citrate, 0.8 mmol/L $NADP^+$, 0.6 mmol/L $MnCl_2$, and 2 units of isocitrate dehydrogenase were added. To allow the indicator metabolites to have access to matrix aconitase, 0.05% lauroyl maltoside (v/v) was added. NADPH formation was photometrically recorded for 10 min.

Diffusion apoptosis slide halo assay. Trevigen's diffusion apoptosis slide halo (DASH) kit allows for an easy discrimination of normal and damaged cells. The method was performed according to the manufacturer's protocol with cells pretreated with thymoquinone 40 μmol/L for 24 h (more details in the supplement).

Cell growth and treatment. Human colon cancer cells HCT116 (p53 −/− and +/+) were cultured in RPMI 1640 supplemented with penicillin (100 units/mL), streptomycin (100 μg/mL), and 10% FCS at 37°C in an atmosphere of 5% CO_2. The HCT116 p53−/− cells were kindly provided by Dr. Carlos Galmarini (Institut National de la Sante et de la Recherche Medicale, Lyon, France). Cells seeded on six-well plates at a density of 10^6 per well were treated with thymoquinone 24 h after plating, and treatment was replenished every 48 h.

Patients. Sporadic colorectal carcinoma specimens were obtained from the Department of Surgery, Medical Faculty Magdeburg, between 1996 and 2005. All aspects of this study were reviewed and approved by the Ethics Committee, and all patients provided informed consent. The tumors were proven to be microsatellite stable as described previously (23). All carcinomas were treated solely by partial colectomy with R0 resection. Tumor and nontumor samples were frozen in liquid nitrogen, stored at −80°C for molecular studies, and formalin-fixed and paraffin-embedded for immunohistochemical analysis. All malignancies were examined by a pathologist, and tumor staging and grading were determined according to the recent guidelines of Union internationale contre le cancer (UICC) tumor-node-metastasis and WHO classification system (24).

Two groups of tumors were investigated: Group A included 20 carcinomas of known p53 mutation status identified in a former study using PCR single-strand conformational polymorphism analysis. Group B comprised 122 carcinomas. Survival data were available for 99 patients. p53 mutation status of tumors in this group was not investigated. Clinicopathologic data of both study groups are given in the supplement.

cDNA array analysis. To identify apoptosis-associated genes that are dysregulated by thymoquinone, we used GEArray Q series Human Apoptosis Gene Array (Superarray Bioscience Corp.) as described recently (25). The complete gene list can be found online.[11]

Real-time reverse transcription-PCR. Real-time reverse transcription-PCR (RT-PCR) was performed as described previously (25). Primer sequences and PCR conditions are given in the supplement.

Protein extraction and immunoblotting. Proteins were prepared as described previously (19). Immunodetection was done using the following primary antibodies: anti-p53 DO1 monoclonal antibody (Oncogene Sc.), anti-CHEK-1 (Santa Cruz Biotechnology), anti–caspase-3 (Cell Signaling), and anti–β-actin (Sigma Aldrich). Details are given in the supplement.

Caspase-3 assay. Caspase-3 activation was measured using the CCP32/caspase-3 fluorometric protease assay kit (Chemicon) as described recently (ref. 26; details in the supplement).

Chromatin immunoprecipitation assay. Chromatin immunoprecipitation (ChIP) assay was carried out in thymoquinone-treated HCT116 p53+/+ cells according to the manufacturer's instructions (Upstate Biotechnologies). CHEK1 promoter primers were sense 5′-AAGCTCCAACATAAACTGCTCGCTTTC-3′ and antisense 5′-GTGCTTTGTAAACCTCAGAGTGCGGTACT-3′ as described previously (7). Details are given in the supplement.

Transient transfection. HCT116 p53−/− cells were transiently transfected with a p53 wild-type (wt) expression vector using Lipofectamine 2000 (Invitrogen) according to the manufacturer's instructions. The expression vector encoding p53-wt was kindly provided by Dr. Y. Haupt (Jerusalem, Israel). Cells were treated with TQ60 24 h following transfection.

Small interfering RNA transfection. SiRNA transfection was performed according to the manufacturer's instructions (Santa Cruz) as described previously (for details, see Supplementary Data; ref. 19).

Tissue microarray. Representative regions of colorectal carcinomas of the study group B were selected on H&E-stained slices for inclusion in a tissue array. More details are given in the supplement.

Immunohistochemistry and terminal deoxyribonucleotide transferase–mediated nick-end labeling assay. For immunohistochemistry, we used the following antibodies: p53 (mouse monoclonal antibody, OP43, dilution 1:30; Oncogene Research Products), CHEK1 (G-4; mouse monoclonal antibody, Santa Cruz Biotechnology), and hMLH1 (mouse monoclonal antibody, G168-15, dilution 1:20, Zymed Laboratories). More details are given in the supplement. Positive immunoreaction of p53 or CHEK1 and positive terminal deoxyribonucleotide transferase–mediated nick-end labeling (TUNEL) reaction was assessed in representative tumor tissue by two different pathologists blinded to clinical data. A tumor was considered positive for p53 accumulation when >5% of the tumor cell nuclei showed definite staining. Cytoplasmic and partly nuclear immunoreaction was recognized for CHEK1. Positive tumor cells were counted. The apoptotic index was determined by counting the number of TUNEL-labeled cells per 100 epithelial cancer cells in 20 fields in the most affected tumor areas under ×400 magnification.

TUNEL assay. TUNEL staining was performed as described previously (23). More details are given in the supplement.

Fluorescence immunostaining analysis. The CHEK1 subcellular localization was carried out on HCT116 p53+/+ and HCT116 p53−/− treated with thymoquinone 60 μmol/L for 48 h and grown on two-well chamber slides (Nunc). CHEK1 was stained with anti-CHEK1 (Santa Cruz Biotechnology) and the nucleus was stained with 4′-6-diamidino-2-phenylindole (DAPI).

Xenograft model. The experiment was performed as described previously (27). Ethical approval was obtained before beginning the experiments (Regional Government of Lower Franconia, Germany). More details are given in the supplement.

Statistical analysis. Statistical analyses were carried out using the χ^2 test in cross tables and one-way ANOVA (for comparison of means) to assess the relationship between immunohistochemical CHEK1 protein expression and clinicopathologic factors. All tests were performed two-sided. To correlate the CHEK1 and p53 or hMLH1 immunohistochemical protein expression levels, we performed Spearman correlation coefficient analysis and the *U* test for independent variables, respectively. Total survival curves were drawn according to the Kaplan-Meier method and compared using the log-rank test. Deaths from unrelated causes were censored. Univariate and multivariate analysis based on Cox's regression analysis was adjusted to test the prognostic relevance of clinicopathologic factors and CHEK1 expression. We used log-linear model and the related χ^2 test for analysis in multivariate contingency tables as well as the configuration frequency analysis for the identification of types and antitypes. $P < 0.05$ was considered statistically significant. Calculations were carried out by SPSS version 13.0 (SPSS, Inc.).

[11] http://www.superarray.com

Results

Thymoquinone induces ROS generation and DNA damage. An early cellular response to double strand breaks is the phosphorylation at Ser^{139} of a subclass of eukaryotic histones, H2A.X (13). TQ at 60 μmol/L caused early and dramatic increase in the amount of H2A.X protein in p53+/+ cells, whereas the amount was slightly increased in the p53−/− cells (Fig. 1*A*). In accordance with these data, DASH assay revealed fewer damaged cells in p53−/− cells (Fig. 1*B*). The changes in H2A.X protein expression and apoptosis were compared with the enhanced oxidative stress in thymoquinone-treated cells. The effect of thymoquinone on mitochondrial superoxide ($O_2^{\cdot-}$) generation was studied with isolated, functionally intact rat liver mitochondria (Fig. 1*C* and *D*). Figure 1*C* shows fluorescence traces indicating the $O_2^{\cdot-}$ mediated oxidation of Amplex red to resorufin. These traces clearly revealed that low concentrations (5–20 μmol/L) of thymoquinone remarkably enhance the generation of ROS. Mitochondrial ROS generation initiated by 20 μmol/L thymoquinone is completely abolished in the presence of catalase, an enzyme decomposing the oxidant H_2O_2. For comparison, Fig. 1*D* shows the increase of ROS generation adjusted by antimycin A (trace 2 μmol/L), an inhibitor of the electron transport respiratory chain, which was used to

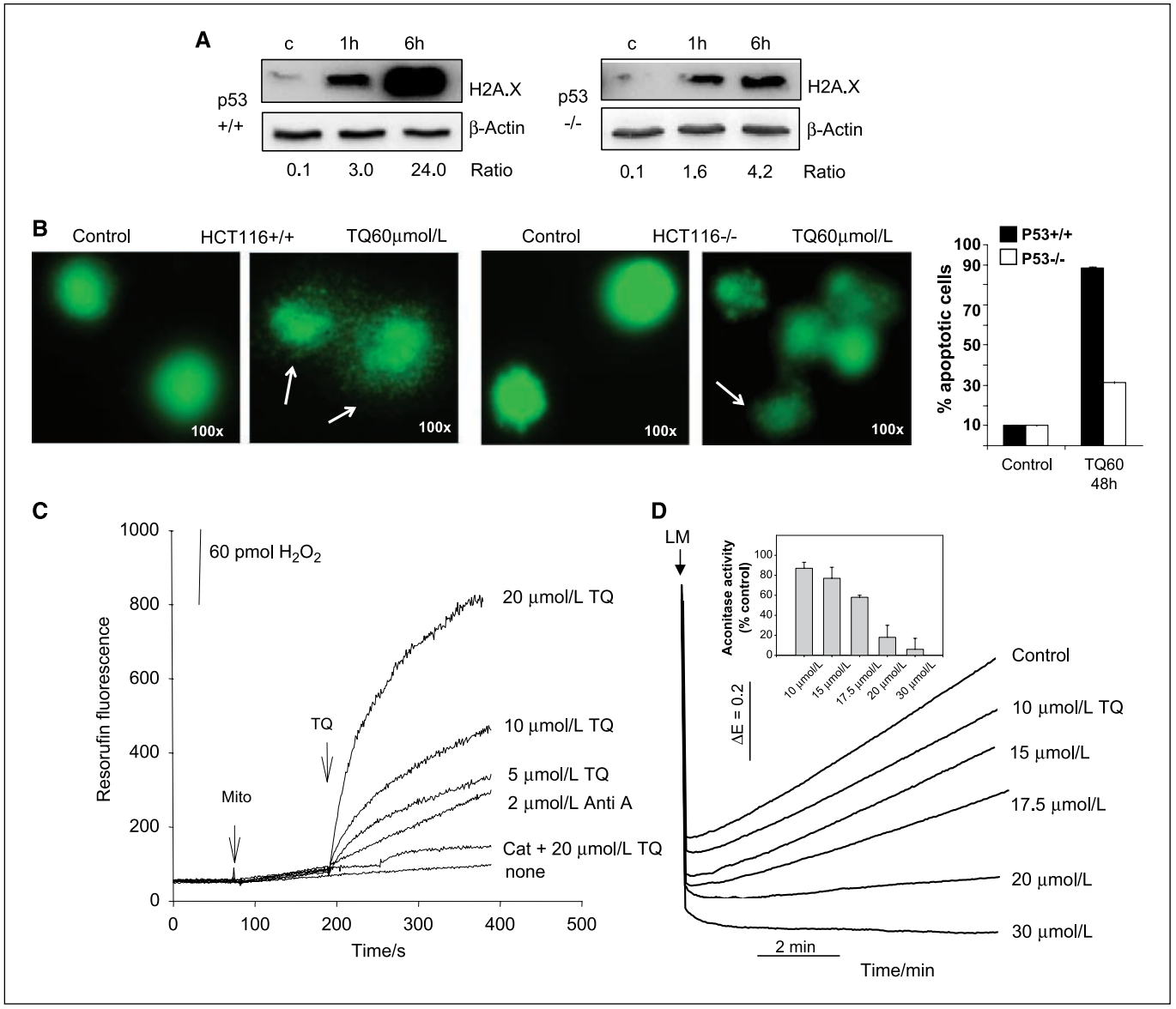

Figure 1. Thymoquinone treatment induced DNA damage in colorectal cancer cells dependent on their p53 status and ROS production by rat liver mitochondria. *A,* 60 μmol/L thymoquinone (*TQ*) induces different DNA damage signals in HCT116 p53+/+ and p53−/− cells reflected by the expression level of H2A.X. *B,* the DASH assay shows the characteristic apoptotic pattern in HCT116 p53+/+ cells, where the alkaline lysis unwinds the DNA in the damaged cells releasing fragments that diffuse away from the center of nucleoid, creating a halo surrounding a small compact region. In HCT116 p53−/− cells, there is a significantly higher number of undamaged cells. *C,* stimulation of mitochondrial ROS production by thymoquinone. Rat liver mitochondria (*Mito*) suspended in incubation buffer were exposed to thymoquinone (2, 5, 10, and 20 μmol/L) or 2 μmol/L of antimycin A (*Anti A*) or 10 μL of catalase (*Cat*) plus 20 μmol/L thymoquinone. The traces show the fluorescence increase. *D,* inactivation of aconitase by thymoquinone-induced mitochondrial ROS production. Rat liver mitochondria were treated first with various concentrations of thymoquinone; thereafter, aconitase activity was measured. Typical traces of aconitase-mediated reduction of $NADP^+$ in mitochondrial samples are shown. *Arrow,* addition of lauroylmaltoside (*LM*). *Inset,* effect of thymoquinone on the aconitase activity. *Columns,* mean obtained with three mitochondrial preparations; *bars,* SD. Activity data of $NADP^+$ reduction are given as min^{-1}.

stimulate ROS. The harmful consequences of thymoquinone-induced ROS generation on the mitochondrial physiology were examined by measuring the aconitase activity, an enzyme of the citric acid cycle that responds to superoxide (22). Figure 1*D* (*inset*) shows that thymoquinone dose dependently inactivates aconitase, suggesting that the enhanced ROS production severely damages the mitochondrial energy metabolism.

Dysregulation of several apoptotic genes in colorectal cancer cells after thymoquinone treatment. We have previously reported that thymoquinone induces apoptosis selectively in HCT116 p53+/+ colorectal cancer cells and this apoptosis was mediated through p53 (18).

To identify thymoquinone-modulated, apoptosis-associated genes, we analyzed the expression of 96 key apoptotic genes using GEArray Q series Human Apoptosis cDNA microarray. We compared HCT116 p53+/+ and HCT116 p53−/− cell lines treated with 60 μmol/L thymoquinone for 48 h. Genes that are up-regulated only in the HCT116 p53−/− cells are likely to be p53 repressed, whereas genes that are up-regulated only in the HCT116 p53+/+ cells are p53 induced. Genes that are dysregulated similarly in both cell lines are thymoquinone-modulated p53-independent genes (Supplementary Table S1). The expression of 17.7% apoptosis-associated genes was modulated by thymoquinone. Analyzing the microarray, it seemed that the most marked difference between drug-treated HCT116 p53+/+ and HCT116 p53−/− cells was the 8.9-fold up-regulation of CHEK1 in HCT116 p53−/− cells, whereas it was 2.5-fold decreased in the HCT116 p53+/+ cells (Supplementary Table S1).

CHEK1 regulation after thymoquinone treatment of HCT116 cells is p53 dependent. To verify the adequacy and status of the CHEK1 mRNA expression and the CHEK1 protein expression, we used real-time RT-PCR and Western blotting, respectively. Both analyses showed that thymoquinone induces a significant down-regulation of CHEK1 mRNA and protein especially at 48 h in HCT116 p53+/+ cells, whereas there was significant induction of CHEK1 in HCT116 p53−/− cells at 48 and 72 h (Fig. 2*A* and *C*). Furthermore, thymoquinone up-regulates p-CHEK1 in HCT116 p53−/− cells but not in HCT116 p53+/+ cells (Fig. 2*B*). This

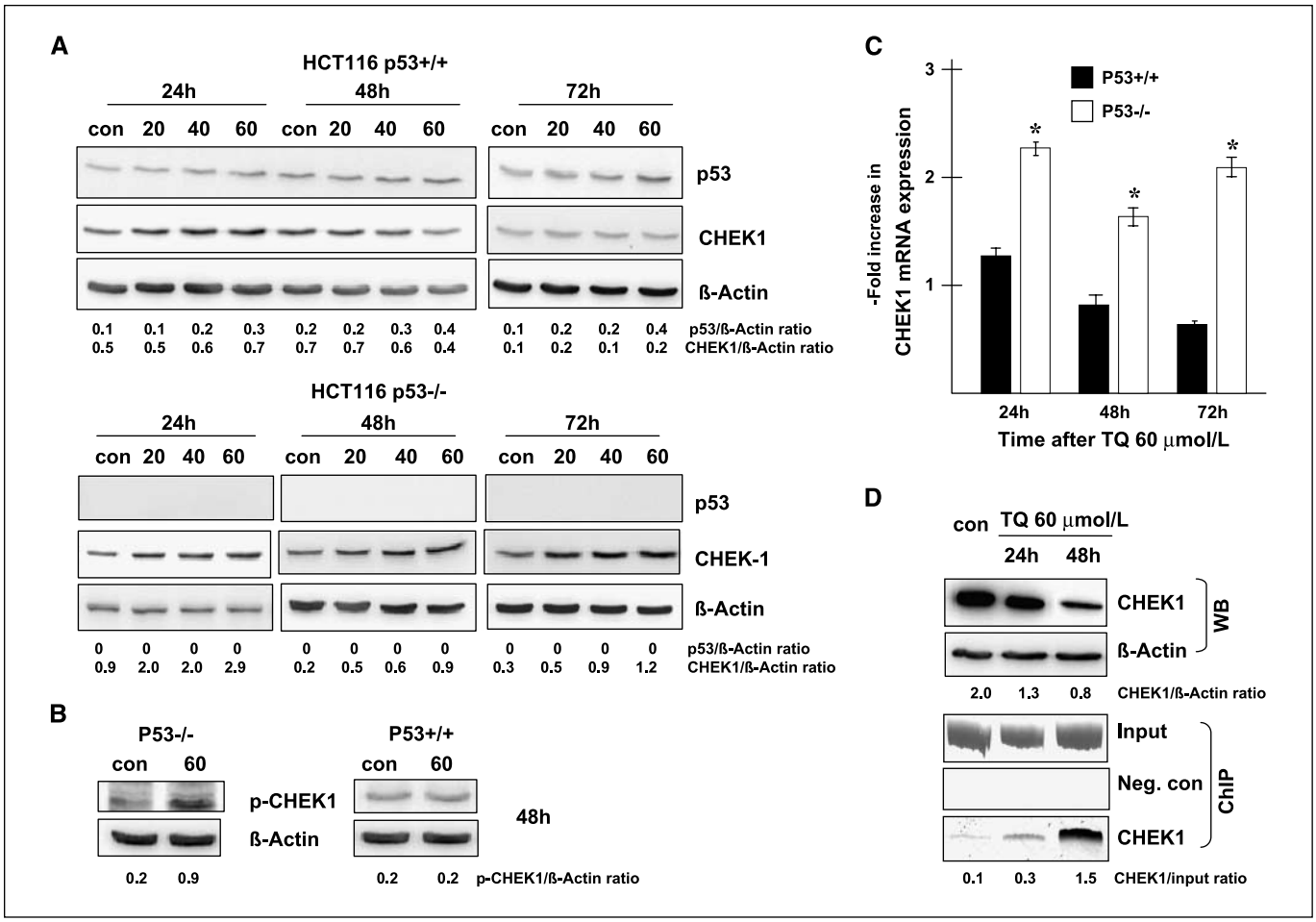

Figure 2. Analysis of p53 and CHEK1 mRNA and protein expression in HCT116 p53+/+ and HCT116 p53−/− cells during thymoquinone treatment. *A,* after thymoquinone treatment (20, 40, and 60 μmol/L), p53 is up-regulated in a time- and dose-dependent manner, whereas CHEK1 protein expression is simultaneously down-regulated in HCT116 p53+/+ cells. In HCT116 p53−/− cells, p53 is not detectable, and CHEK1 is up-regulated after thymoquinone treatment. Fold expression changes are given below the blots. *B,* after 48 h, thymoquinone 60 μmol/L up-regulates p-CHEK1 in HCT116 p53−/− cells but not in the HCT116 p53+/+ cells. *C,* up-regulation of CHEK1 in HCT116 p53−/− cells occurred at the transcriptional level shown for thymoquinone 60 μmol/L: The ratio of CHEK1/β2-microglobulin after thymoquinone treatment versus control ratio was set at 1.0 (*, thymoquinone treatment at all three time points was statistically significant against the control for $P < 0.01$). *Columns,* mean from three experiments; *bars,* SD. ChIP assay using p53 antibody confirmed that there is transcriptional repression of CHEK1 expression after thymoquinone treatment in p53+/+ cells. Two controls were included: the input control (*Input*) and a negative control ChIP (*Neg. con*) without using the p53 antibody. CHEK1 protein amount (*WB*, Western blotting) decreases with stronger binding of p53 at the CHEK1 promoter (*D*).

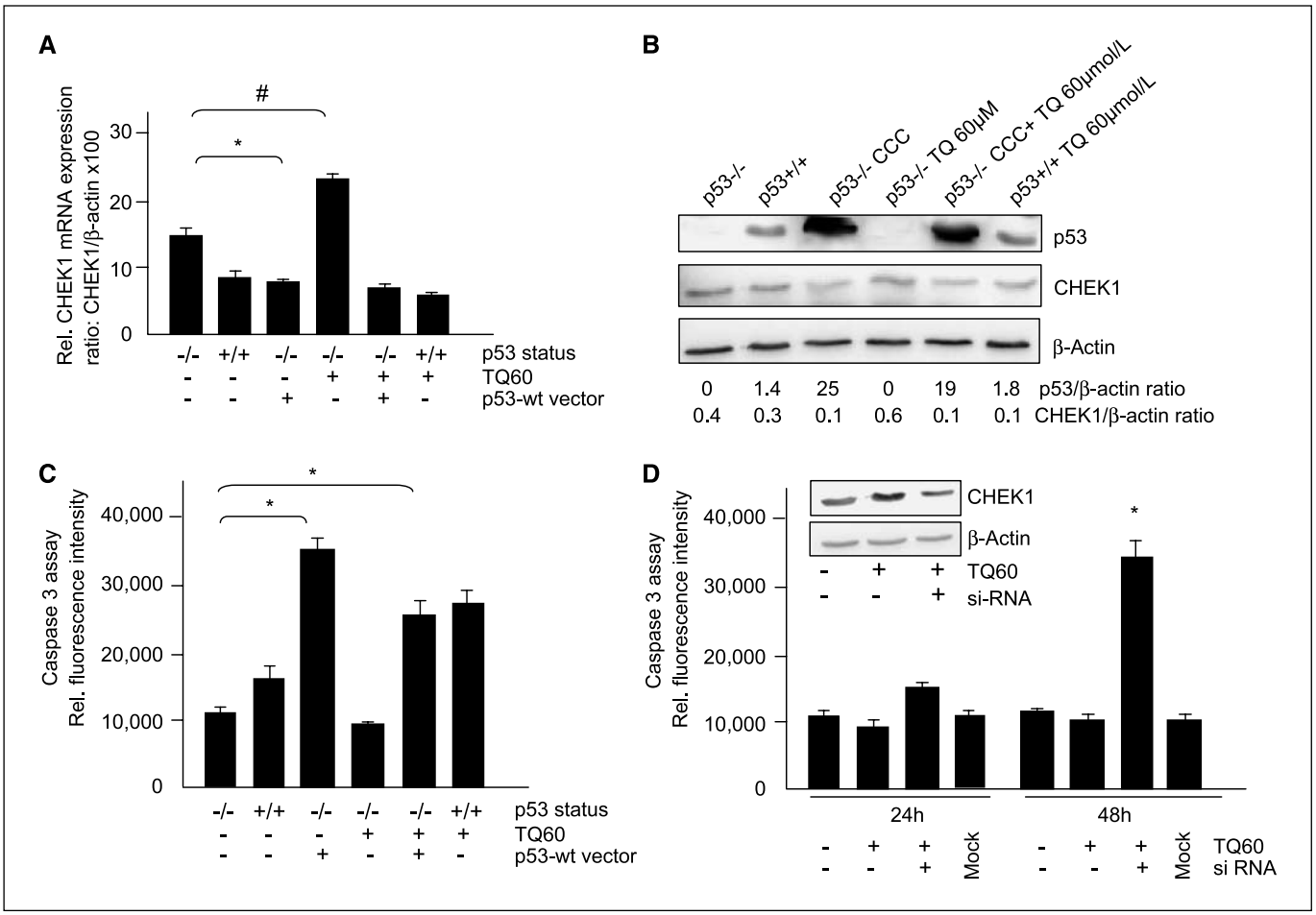

Figure 3. Association between p53/CHEK1 level and caspase-3 activity in HCT116 p53+/+ and p53−/− cells. Thymoquinone 60 μmol/L treatment (*TQ60*, 48 h) induced CHEK1 mRNA expression in p53−/− cells (#, $P < 0.01$). Transfection of p53−/− cells with a p53-wt vector (*CCC*) significantly reduced the amounts of CHEK1 transcripts (*, $P < 0.01$; *A*) and protein (*B*) and enhanced their caspase-3 activity (*, $P < 0.01$; *C*). Thymoquinone treatment of p53-wt–transfected p53−/− cells did not further decrease CHEK1 mRNA (*A*) or protein expression (*B*), nor did it increase caspase-3 activity (*C*). Knockdown of CHEK1 by siRNA reduced CHEK1 protein by 65% (*inset, D*) and significantly enhanced the caspase-3 activity after 48 h of thymoquinone treatment (*, $P < 0.01$; *D*). The mock control did not influence CHEK1 protein levels (data not shown) or caspase-3 activity levels. *Columns,* mean of three experiments; *bars,* SD.

indicates that p53 status directly influences CHEK1 expression in response to thymoquinone.

p53 interacts directly with CHEK1 promoter. CHEK1 is directly repressed by p53 after treatment of HCT116 cells with the anticancer drug 5-fluorouracil (7). To determine whether CHEK1 down-regulation is due to direct transcriptional repression by p53 promoter binding, we used p53 antibody to immunoprecipitate chromatin from HCT116 p53+/+ cells treated with the drug. The ChIP assay showed that the genomic fragment containing p53 binding site from CHEK1 promoter was enriched during the course of treatment, reaching 3-fold after 24 h and 15-fold after 48 h (Fig. 2*D*). The level of p53 binding inversely correlated with the accumulation of CHEK1 RNA transcripts (Fig. 2*C*) and CHEK1 protein (Fig. 2*D*). This suggests that the down-regulation of CHEK1 protein may be partly caused by p53 binding at the CHEK1 promoter.

Both recovery of p53 function and knockdown of CHEK1 in p53−/− cells sensitize them to apoptosis. To gain further insight into whether p53-dependent down-regulation of CHEK1 contributes to apoptosis after thymoquinone treatment (TQ60, 48 h), we transfected HCT116 p53−/− cells with p53-wt containing plasmid vector to restore p53 levels. Indeed, p53−/− cells transfected with p53-wt showed nearly the same low amount of CHEK1 mRNA (Fig. 3*A*) and protein expression (Fig. 3*B*) as observed in p53+/+ cells. After drug treatment, the CHEK1 mRNA and protein expression was 20% higher in p53−/− cells compared with transfected cells (Fig. 3*A* and *B*). The transient overexpression of p53 substantially enhanced caspase-3 activity (2.5-fold; Fig. 3*C*). Transfection of p53−/− cells with an empty vector caused no significant caspase-3 activation (data not shown).

To study the role of CHEK1 in thymoquinone-induced apoptosis, we transfected p53−/− cells with CHEK1 siRNA (Fig. 3*D*). Immunoblotting showed that CHEK1 protein was reduced by 60% in transfected cells (Fig. 3*D, inset*). Caspase-3 activity reached ~2-fold higher levels than in p53+/+ cells (Fig. 3*C* and *D*).

Our data suggest that the repression of CHEK1 expression by thymoquinone may prevent cells from progressing through a prosurvival pathway.

p53-dependent CHEK1 repression is evident in human colorectal cancer tissues and is accompanied by enhanced apoptosis. In an attempt to use an *in vivo* model to validate our *in vitro* findings, we investigated CHEK1 levels in a panel of human colon cancer tissues that are well characterized for p53 mutation status and for immunohistochemical p53 protein expression (study

group A). We used two types of tumors that differ in their p53 status. The first group included tumors bearing p53 frameshift mutations (deletion or insertion, legend of Fig. 4) resembling the HCT116 p53−/− cells. The second group consisted of tumors with p53-wt resembling the HCT116 p53+/+ cells. The first group showed loss of p53 mRNA expression (Fig. 4*A*) and p53 protein expression in immunohistochemistry (data not shown) and Western blotting (Fig. 4*C*). p53-wt tumors were negative in Western blotting and weakly expressed p53 protein in only a few tumor nuclei using immunohistochemical staining. Although available, p53 protein was undetectable because of its short half life, but p53 mRNA expression was detectable (Fig. 4*A*). Confirming the *in vitro* findings, p53-wt tumors showed lower CHEK1 mRNA expression [average ratio CHEK1/β2-microglobulin, 0.31 (0.1–2.5); Fig. 4*B*] compared with the p53-deleted tumors [average ratio CHEK1/β2-microglobulin, 6.39 (3.1–8.9)]. p53-deleted tumors showed higher amounts of CHEK1 protein [average ratio, 1.4 (0.8–2.7)] compared with p53-wt tumors [average ratio, 0.4 (0.2–0.6); Fig. 4*C*]. Using TUNEL, we showed that p53-wt tumors had higher number of apoptotic cells than tumors bearing a truncated p53 protein (Fig. 4*D*).

p53-dependent CHEK1 repression in mouse xenografts enhances drug sensitivity. We have previously reported that thymoquinone delays the growth of HCT116 p53+/+ mouse xenografts (27). By contrast, in this study, the growth of p53−/− xenografts was nearly unaffected by thymoquinone treatment after 14 days of injection (p53+/+ cells: control 20.2 mm ± 1.2, thymoquinone 14.2 mm ± 1.4; p53−/− cells: control 13.1 ± 1.1, thymoquinone 12.6 mm ± 0.5). To determine if the *in vivo* sensitivity of p53+/+ xenografts to thymoquinone was due to p53-dependent CHEK1 repression, we characterized the xenograft tissues for CHEK1 protein expression levels. Indeed, p53+/+ xenografts showed a significantly lower CHEK1 expression compared with the p53−/− ones (Fig. 5*A* and *C*). To assess if the differential growth delay was related to apoptosis, we performed TUNEL staining of tissues and caspase-3 cleavage by Western blotting. Again, p53−/− cells having the highest amounts of CHEK1 protein showed the lowest signs of apoptosis (Fig. 5*C* and *D*; Supplementary Fig. S1). These data provide compelling evidence for the involvement of the stress response sensor CHEK1 in thymoquinone-induced apoptosis.

Furthermore, in xenograft tissues of p53−/− cells, thymoquinone resulted in a stronger nuclear shift of CHEK1 protein expression, whereas in untreated (p53−/− or p53+/+) cells, a weak nuclear expression of CHEK1 was detected (Fig. 5*A*). Coimmunofluorescence analysis of HCT116 cells grown on coverslips showed an increase in CHEK1 protein expression in the cytoplasm as well as in the nucleus of p53−/− cells after thymoquinone treatment,

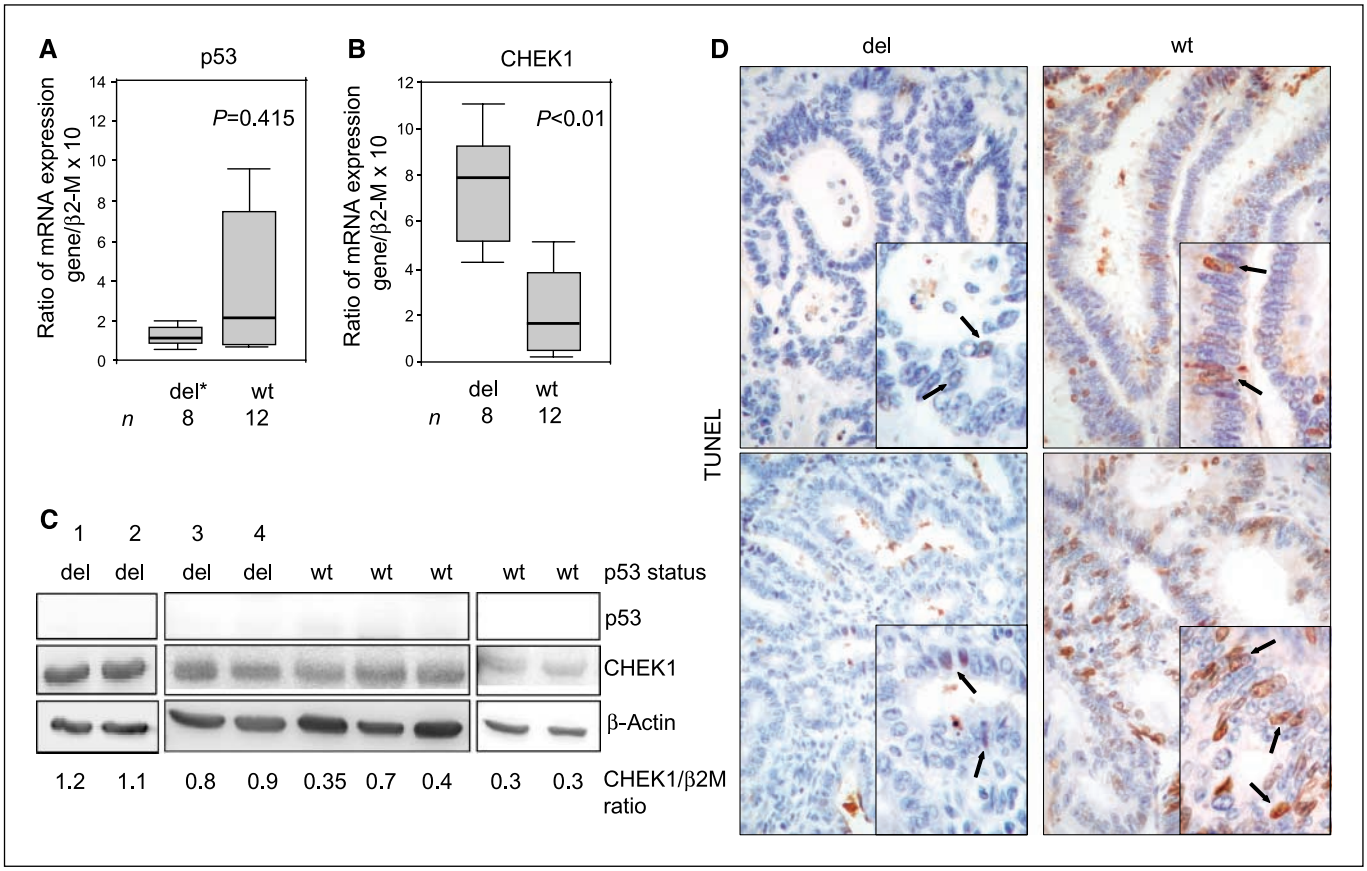

Figure 4. Comparison of the expression of p53 and CHEK1 proteins in p53−/− (del*) and p53-wt human colorectal carcinomas (study group A). Whereas the p53 mRNA expression did not differ between both tumor groups (*A*), a significantly higher CHEK1 mRNA expression was detected in the p53−/− (del) tumors compared with the p53-wt tumors (*B*). There was no visible p53 band in the p53−/− and p53-wt samples in the immunoblot, but a higher CHEK1 protein expression was found in the p53−/− tumors compared with low CHEK1 expression in the p53-wt tumors (*C*). *, detailed information about the p53 mutations: case 1 (exon 5, codon 146, 1-bp insertion), case 2 (exon 7/splice acceptor, 12-bp deletion), case 3 (exon 4, codon 93, C-deletion/ stop-codon in exon 4), case 4 (exon 6, codon 190, 5-bp deletion/stop-codon in exon 7). TUNEL staining of p53−/− (del) tumors revealed a remarkably lower number of TUNEL-positive nuclei (*arrows*) compared with p53-wt tumors; two examples are given (magnifications: ×100, ×10; *insets,* ×400, ×4; *D*).

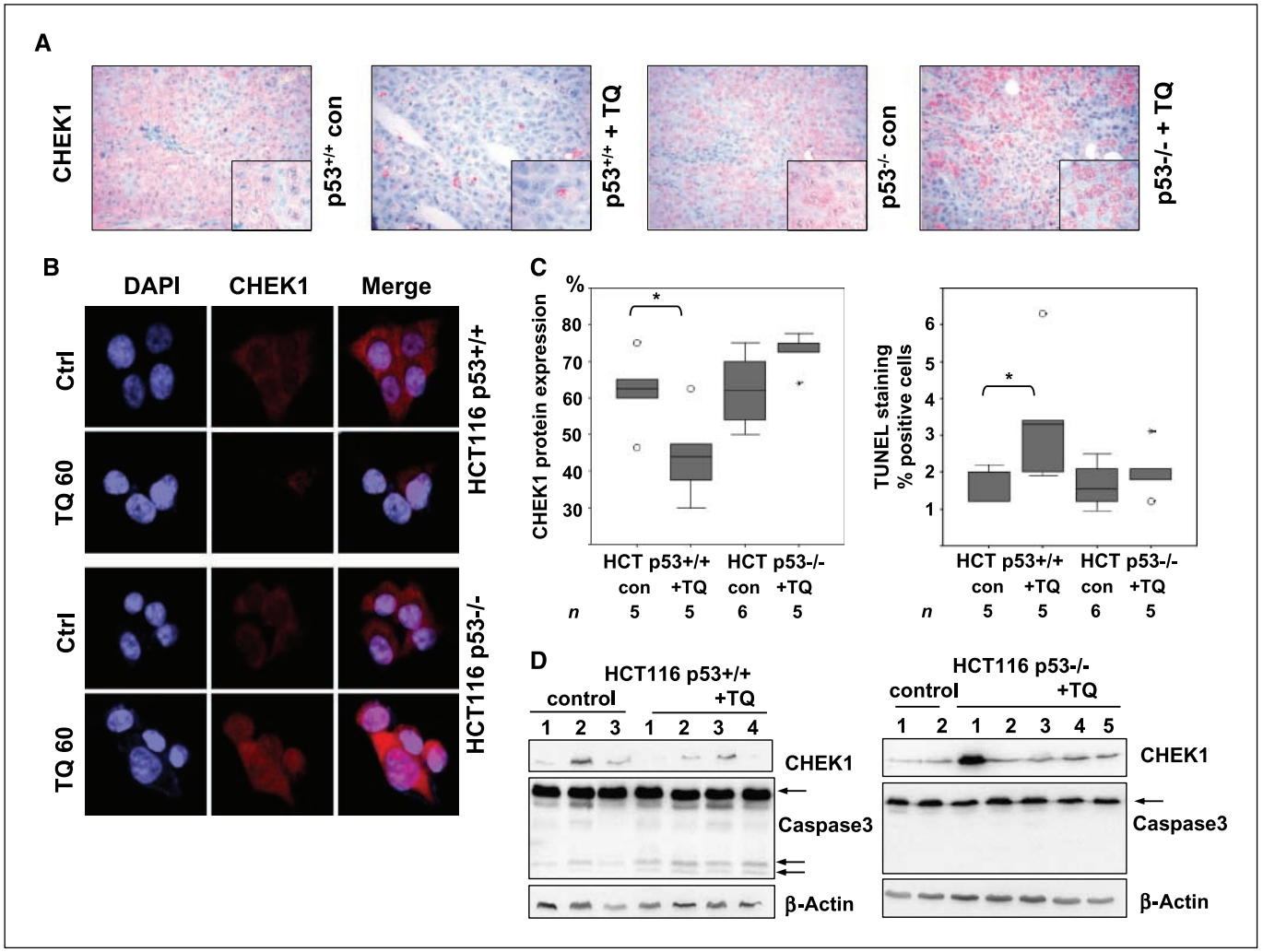

Figure 5. Analysis of p53 and CHEK1 expression in mouse xenograft tissues and correlation with apoptosis. *A,* light microscopic images (×200 magnification) of immunohistochemistry for CHEK1 and CHEK1 subcellular localization in p53+/+ and p53−/− tumors after thymoquinone treatment. Specimens obtained from p53−/− cells (*con,* control) strongly express CHEK1 protein with a further increase and simultaneous occurrence of nuclear shuttling after drug treatment (enlargements in *A*). Specimens with p53-wt status (*con,* control) show high CHEK1 protein expression; drug treatment resulted in a remarkable reduction of CHEK1 immunostaining without nuclear signals. *B,* we confirmed the nuclear shuttling of CHEK1 after thymoquinone treatment in HCT116 p53−/− cells using fluorescence immunostaining. Cells were fixed in 3% paraformaldehyde for 15 min and permeabilized with 0.2% Triton X-100 for 5 min. After blocking with 1% bovine serum albumin for 10 min, they were incubated with mouse anti-CHEK1 antibody overnight at 4°C, followed by incubation with Cy3 anti-mouse secondary antibody (Sigma). The slides were counterstained and mounted with DAPI (Vector Labs) and were examined using Axioplan2 (Zeiss) fluorescent microscope. *C,* box plot analysis showing the percentage of CHEK1-expressing tumor cells (*left*) and of TUNEL-positive apoptotic cells (*right*) in mouse xenografts after thymoquinone treatment. The number of investigated mouse tissues is given below the graph. *D,* Western blotting for CHEK1 and caspase-3 cleavage in mouse xenografts confirmed that p53−/− cells significantly up-regulated the protein amount of CHEK1 and did not undergo apoptosis after thymoquinone treatment. Thymoquinone did not induce CHEK1 protein expression but induced caspase-3 cleavage in p53+/+ colon cancer cells. The number of animals is given above the gel image.

whereas in the p53+/+ cells CHEK1 nearly disappeared and was not visible in the nucleus of tumor cells. Our data suggest that, in the absence of p53, thymoquinone causes the shuttling of CHEK1 into the nucleus (Fig. 5*B*).

CHEK1 overexpression has a prognostic effect on sporadic colorectal cancer patients. Immunohistochemical protein expression of CHEK1, p53, and hMLH1 was investigated in a group of sporadic colorectal carcinomas (study group B) and corresponding nontumor colon tissue grouped in a tissue microarray (Fig. 6*A*). According to the ROC curve, an optimal balance between sensitivity (68.3%) and specificity (61.4%) was reached at 60% positivity for CHEK1 expression (Fig. 6*B*). Sixty of 122 carcinomas (50.8%) showed cytoplasmic CHEK1 expression in >60% of the tumor cells and were considered as CHEK1-overexpressing tumors (Fig. 6*A*). CHEK1 overexpression correlated significantly with tumor localization (P = 0.02); distal tumors more frequently overexpressed CHEK1. This was confirmed by the multivariate configuration table. It revealed two "types" that reflected the overrepresented combinations of the following variables. Type 1: CHEK1 low, alive, proximal tumor localization; type 2: CHEK1 overexpression, died of disease, distal tumor localization (P < 0.004, Table 1). CHEK1 overexpression was correlated with advanced tumor stages (Fig. 6*C*; P = 0.03). There was no association between CHEK1 expression and other clinicopathologic factors such as sex, tumor size, lymph node metastases, tumor grading, and age. There was no correlation between CHEK1 and p53 protein expression (Spearman correlation coefficient: $r_s = -0.045$, P = 0.674) as well as between CHEK1 and hMLH1 immunostaining (U test, P = 0.828).

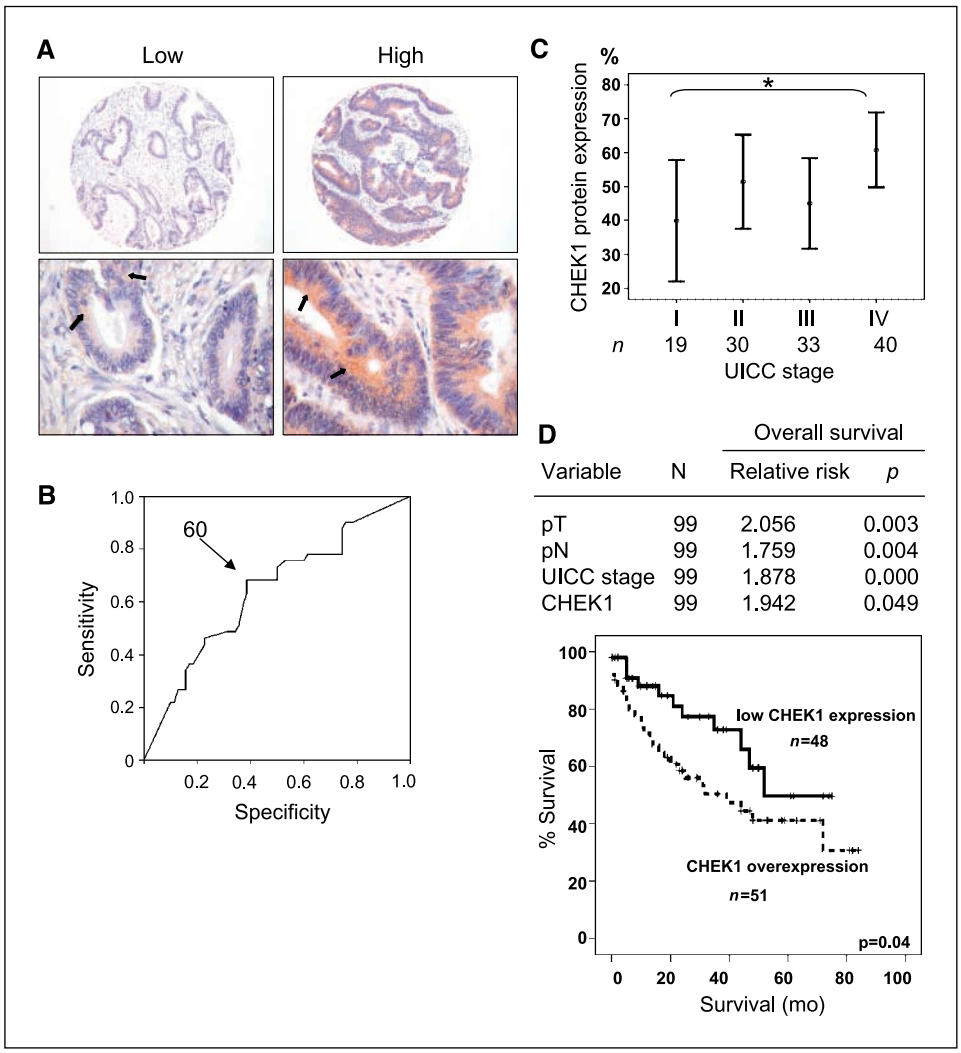

Figure 6. Analysis of CHEK1 expression in sporadic colorectal cancer and survival analysis (study group B). *A,* light microscopic images (upper row × 100, lower row × 400 magnification) of immunohistochemistry for CHEK1 on colorectal cancer tissue. Representative samples of both low expression and overexpression of CHEK1 are given. *B,* the receiver operating curve plot revealed an optimal balance in sensitivity (68.3%) and specificity (61.4%) at 60% positivity for CHEK1 expression. Thus, a cutoff at 60% positivity (≤60%) for CHEK1 protein expression was considered as "overexpressed" and used for survival analysis. *C,* CHEK1 overexpression was correlated significantly with higher tumor staging. In the univariate Cox regression analysis, tumor size (pT), lymph node status (pN), UICC stage, and CHEK1 expression had prognostic significance. *D,* the Kaplan-Meier plot for survival as a function of CHEK1 expression revealed that the patient group with CHEK1-overexpressing tumors displayed the worst clinical outcome. *mo*, months.

Patients who had CHEK1-overexpressing tumors had a worse prognosis than those having tumors with low CHEK1 expression. After 5 years, patients affected by tumors with CHEK1 overexpression and those without had overall survivals of 49% and 30.8%, respectively. Twenty-seven of 54 patients (50%) with CHEK1-overexpressing tumors but only 14 of 57 patients (24.6%) with CHEK1-low expressing tumors died of disease ($P = 0.006$; Fig. 6*D*). There was a high predictive value for CHEK1 overexpression and clinical outcome. Univariate Cox regression analysis revealed 1.95-fold increased risk of dying of disease in the CHEK1-overexpressing tumor group (Fig. 6*D*). All four factors that were significant in the univariate analysis were included in the multivariate test for independency. Only UICC staging, pT, and CHEK1 expression retained their strong independent prognostic value ($P < 0.01$). In normal colon mucosa, nuclear expression of CHEK1 protein was detected with attenuation of the crypt base (Supplementary Fig. S2).

Discussion

In a genome-wide scale, p53 was shown to induce apoptosis through transcriptional activation of its putative apoptotic targets (e.g., PUMA, NOXA, PIG3, Fas/CD95). However, there is indirect evidence that p53 also induces apoptosis through transcriptional repression of antiapoptotic signals (e.g., PLK, PTTG1, CHEK1; refs. 7, 28). The mechanisms of p53-mediated repression and its involvement in apoptosis are poorly understood.

By comparing the gene expression profiles of HCT116 p53+/+ and their p53-null counterparts after thymoquinone treatment, we attempted to identify p53-dependent target genes that could explain the differential sensitivity of these cells to drug-induced apoptosis. CHEK1 was chosen for further investigation, as it was 9-fold up-regulated by thymoquinone in HCT116 p53−/− cells. Here, we show that p53 protein represses the expression of CHEK1 in HCT116 p53+/+ cells. Recently, it was reported that p53 transactivates CHEK1 expression through binding to a putative p53-responsive element in the CHEK1 promoter between nucleotides −1429 to −1169 (7). In response to thymoquinone, p53 binding occurred at the CHEK1 promoter in HCT116 cells as revealed by ChIP assay. The tested genomic fragment containing the p53 binding site from the CHEK1 promoter (7) was enriched after ChIP, which is in accordance with the down-regulation in CHEK1 protein expression. Using a panel of human colon cancer tissues well-characterized for p53 mutation status, we confirmed the *in vitro* findings in human tumors *in vivo* and showed that p53 mutations, resulting in a truncated nonfunctional p53 protein, had

significantly higher amounts of CHEK1 mRNA and protein. This was accompanied by poor caspase-3 activation when compared with p53-wt–expressing colon carcinomas. Further evidence for the involvement of CHEK1 down-regulation in drug-induced apoptosis was shown by our mouse xenograft study (27). We found that tumor growth was significantly inhibited by thymoquinone in HCT116 p53+/+ xenografts, which may be attributed to the induction of apoptosis as indicated by TUNEL positivity and caspase-3 cleavage. Thymoquinone-induced tumor growth delay was diminished in the p53−/− xenografts. We observed p53-dependent subcellular localization of CHEK1 with lack of nuclear staining in p53+/+ cells after thymoquinone treatment. In contrast, we did not find any differences in subcellular localization of CHEK1 in both untreated HCT116 p53+/+ and p53−/− control cells, as well as in p53-null and p53-wt human tumors. Considering both the xenograft findings and the results of the *in vitro* immunofluorescence staining, showing CHEK1 in the nucleus after thymoquinone treatment, we suggest that nuclear shuttling of CHEK1 occurs only in response to thymoquinone.

Two different pathways have been implicated in viability following DNA damage, the CHEK1/CHEK2 pathway and the $p53/p21^{WAF1}$ pathway (29, 30). According to earlier studies (18), thymoquinone induced G_1-S arrest in HCT116 p53+/+ colorectal cancer cells. p53−/− cells, which are defective in G_1 arrest, rely more strongly on the S or G_2 checkpoint to repair their damaged DNA when treated with genotoxic drugs (14). Indeed, after thymoquinone treatment, a significant proportion of HCT116 p53−/− cells arrested in the S phase (data not shown).

CHEK1 seems to play a role in the cross-talk between the mechanisms that drive apoptosis and those that control the cell cycle. It seems to prevent cells bearing damaged DNA from progressing through the cell cycle, which would lead to an unsuccessful and lethal attempt to undergo cell division (15, 31). In agreement with a CHEK1 antiapoptotic role, conditional CHEK1 knockout mice showed severe cell death in proliferating somatic cells (32). An antiapoptotic role for CHEK1 in response to replication fork stresses was recently reported (33). To determine whether CHEK1 down-regulation contributes to enhanced apoptosis in p53-wt cells, we evaluated the apoptotic response of p53−/− cells after transfection with p53-wt plasmid. The level of caspase-3 activity in transfected p53−/− cells was restored to that of p53-wt cells. The knockdown of CHEK1 in p53−/− cells by siRNA led to enhanced caspase-3 activity in response to thymoquinone. We are aware that no target of p53 will suffice to recapitulate the p53-dependent apoptosis phenotype under all physiologic circumstances. In certain tissues and under conditions of stress development, some p53 targets may be required for apoptosis.

In accordance with other studies, we showed that thymoquinone is a potent inducer of mitochondrial $O_2^{\cdot-}$ generation. This finding can be explained by two properties of thymoquinone: (*a*) a high solubility in the lipid core of the inner mitochondrial membrane and (*b*) an easy reduction of thymoquinone to its semireduced form. It seems that thymoquinone enhances the superoxide generation after its incorporation in the respiratory chain by increasing the capacity of complex III for the one-electron transfer reaction to molecular oxygen. The stimulation of $O_2^{\cdot-}$ generation by thymoquinone can be because it is chemically related to ubiquinone, ultimately leading to the development of peroxide. This suggests that the semireduced thymoquinone increases the capacity of one-electron transitions to molecular oxygen. A recent report indicated that the half-reduced form of ubiquinone, semiubiquinone, is a critical site of the one-electron transfer to molecular oxygen, thereby forming the superoxide radical (34). The observation that thymoquinone acts as a potent inducer of mitochondrial ROS suggests that it initiates oxidative stress inside cells. Mitochondria are likely to be also the target of the harmful effects of ROS, which eventually leads to apoptosis. Our study of osteosarcoma cells indicated that thymoquinone induces apoptosis through the cleavage of caspase-3 and caspase-9 (19). Furthermore, the ability of thymoquinone to induce DNA damage in colorectal cancer cells points to the possibility that such damage may be the key factor for the activation of CHEK1 damage checkpoint.

To date, only two recent studies have reported on CHEK1 expression in cancer (35, 36). Investigating a group of Korean colorectal cancer patients, they showed that *CHEK1* gene had more functionally inactivating frameshift mutations in patients with microsatellite instability. These mutations lead to a defective DNA damage response. In a study of human breast cancer, CHEK1 overexpression was significantly correlated with higher tumor grade (36). These authors confirmed an E2F-dependent transactivation of the CHEK1 promoter *in vitro* and *in vivo*. We show for the first time a correlation between CHEK1 overexpression and tumor malignancy and a worse

Table 1. Multivariate contingency table for evaluating the prognostic link between CHEK1 overexpression and tumor localization

DOD	Localization	CHEK1	Observed	Expected	*P*
No	Proximal	No	21	12.63	0.02 ← type
No	Proximal	High	7	11.96	0.15
No	Distal	No	22	23.32	0.79
No	Distal	High	20	22.09	0.66
Yes	Proximal	No	5	7.40	0.38
Yes	Proximal	High	6	7.01	0.70
Yes	Distal	No	9	13.66	0.21
Yes	Distal	High	21	12.94	0.03 ← type

NOTE: ←, overrepresented variable combination defined as "type" ($P < 0.004$).
Abbreviation: DOD, died of disease.

prognosis, respectively, in colorectal tumors. This seems to be of great clinical interest because it has been suggested that inhibition of checkpoint signaling, especially by CHEK1 inhibitors, may correlate with the effectiveness of cancer treatment (37). The higher frequency of CHEK1-overexpressing tumors in distal tumor localization is in accordance with the observation that distal tumors also show a higher number of p53 mutations (38). Even so, it was not surprising that CHEK1 protein expression did not correlate with p53 protein expression in tumors, because p53-wt and p53-null tumors cannot be differentiated by immunohistochemistry. In addition, we have no data available whether different p53 mutants are able to repress CHEK1 differently. CHEK1 overexpression does not seem to be correlated with the chromosomal instability group as shown by a lack of correlation between CHEK1 and hMLH1 immunostaining.

In summary, p53-dependent CHEK1 inhibition as shown by the action of thymoquinone seems to be a general mechanism responsible for apoptosis induction in colorectal cancer. Our data confirm the existence of a CHEK1/p53 link and its prognostic significance in human colorectal cancer tissues. Because colon cancers harbor p53 mutations in >50% of cases and CHEK1 activation lowers the efficacy of DNA-damaging drugs, we believe that thymoquinone, in combination with CHEK1 inhibitors, may be therapeutically promising for colorectal cancer.

Disclosure of Potential Conflicts of Interest

No potential conflicts of interest were declared.

Acknowledgments

Received 3/7/2008; revised 4/28/2008; accepted 4/29/2008.

Grant support: Deutsche Forschungsgemeinschaft (SCHN477-1-4) and ELAN program for Research and Teaching (University Hospital Erlangen, 07.03.30.1). C. Habold, M. Diab-Assaf, and W. Itani were supported by the German Academic Exchange Service.

The costs of publication of this article were defrayed in part by the payment of page charges. This article must therefore be hereby marked *advertisement* in accordance with 18 U.S.C. Section 1734 solely to indicate this fact.

References

1. Lakin ND, Jackson SP. Regulation of p53 in response to DNA damage. Oncogene 1999;18:7644–55.
2. Vogelstein B, Lane D, Levine AJ. Surfing the p53 network. Nature 2000;408:307–10.
3. Rozan LM, El-Deiry WS. P53 downstream target genes and tumor suppression: a classical view in evolution. Cell Death Differ 2007;14:3–9.
4. Bhonde MR, Hanski ML, Notter M, et al. Equivalent effect of DNA damage-induced apoptotic cell death or long-term cell cycle arrest on colon carcinoma cell proliferation and tumour growth. Oncogene 2006;25:165–75.
5. Brugarolas J, Chandrasekaran C, Gordon JI, et al. Radiation-induced cell cycle arrest compromised by p21 deficiency. Nature 1995;377:552–7.
6. Ko LJ, Prives C. P53: puzzle and paradigm. Genes Dev 1996;10:1054–72.
7. Kho PS, Wang Z, Zhuang L, et al. P53-regulated transcriptional program associated with genotoxic stress-induced apoptosis. J Biol Chem 2004;279:21183–92.
8. El-Deiry WS. Regulation of p53 downstream genes. Semin Cancer Biol 1998;8:345–57.
9. Sun Y. P53 and its downstream proteins as molecular targets of cancer. Mol Carcinog 2006;45:409–15.
10. Ho J, Benchimol S. Transcriptional repression mediated by the p53 tumour suppressor. Cell Death Differ 2003;10:404–8.
11. Damia G, Sanchez Y, Erba E, Broggini M. DNA damage induces p53-dependent down-regulation of hCHK1. J Biol Chem 2001;276:10641–5.
12. Shiloh Y. ATM and related protein kinases: safeguarding genome integrity. Nat Rev Cancer 2003;3:155–68.
13. Tse AN, Carvajal R, Schwartz GK. Targeting checkpoint kinase 1 in cancer therapeutics. Clin Cancer Res 2007;13:1955–60.
14. Xiao Z, Chen Z, Gunasekera AH, et al. Chk1 mediates S and G_2 arrests through Cdc25A degradation in response to DNA-damaging agents. J Biol Chem 2003;278:21767–73.
15. Xiao D, Herman-Antosiewicz A, Antosiewicz J, et al. Diallyl trisulfide-induced G(2)-M phase cell cycle arrest in human prostate cancer cells is caused by reactive oxygen species-dependent destruction and hyperphosphorylation of Cdc 25 C. Oncogene 2005;24:6256–68.
16. Zhao B, Bower MJ, McDevitt PJ, et al. Structural basis for Chk1 inhibition by UCN-01. J Biol Chem 2002;277:46609–15.
17. Maude SL, Enders GH. Cdk inhibition in human cells compromises chk1 function and activates a DNA damage response. Cancer Res 2005;65:780–6.
18. Gali-Muhtasib H, Diab-Assaf M, Boltze C, et al. Thymoquinone extracted from black seed triggers apoptotic cell death in human colorectal cancer cells via a p53-dependent mechanism. Int J Oncol 2004;25:857–66.
19. Roepke M, Diestel A, Bajbouj K, et al. Lack of p53 augments thymoquinone-induced apoptosis and caspase activation in human osteosarcoma cells. Cancer Biol Ther 2007;6:160–9.
20. Nohl H, Gille L, Kozlov AV. Prooxidant functions of coenzyme Q. In: Fat-soluble vitamins. 1st ed. Norwell (MA): Kluwer Academic Pub; 1998. p. 509–24.
21. Steinbrecht I, Kunz W. Use of "cycling" technique for random quantitative determination of the degree of reduction of NAD and NADP system in rat liver mitochondria with continuous recording of the measurements. Acta Biol Med Ger 1970;25:731–47.
22. Gardner PR. Aconitase: sensitive target and measure of superoxide. Methods Enzymol 2002;349:9–23.
23. Schneider-Stock R, Kuester D, Ullrich O, et al. Close localization of DAP-kinase positive tumour-associated macrophages and apoptotic colorectal cancer cells. J Pathol 2006;209:95–105.
24. Sobin LH, Wittekind C. TNM classification of malignant tumours. 6th ed. New Jersey: John Wiley & Sons; 2002. p. 272.
25. Schneider-Stock, R, Diab-Assef M, Rohrbeck A, et al. 5-Aza-cytidine is a potent inhibitor of DNA methyltransferase 3a and induces apoptosis in HCT-116 colon cancer cells via Gadd45- and p53-dependent mechanisms. J Pharmacol Exp Ther 2005;312:525–36.
26. Habold C, Poehlmann A, Bajbouj K, et al. Trichostatin A causes p53 to switch oxidative-damaged colorectal cancer cells from cell cycle arrest into apoptosis. J Cell Mol Med 2008;12:607–21.
27. Gali-Muhtasib H, Ocker M, Kuester D et al. Thymoquinone reduces mouse colon tumor cell invasion and inhibits tumor growth in murine colon cancer models. J Cell Mol Med 2008;12:330–42.
28. Mirza A, Wu Q, Wang L, et al. Global transcriptional program of p53 target genes during the process of apoptosis and cell cycle progression. Oncogene 2003;22:3645–54.
29. Taylor WR, Stark GR. Regulation of the G_2/M transition by p53. Oncogene 2001;20:1803–15.
30. Broude EV, Demidenko ZN, Vivo C, et al. p21 (CDKN1A) is a negative regulator of p53 stability. Cell Cycle 2007;6:1468–71.
31. Chen Z, Xiao Z, Gu WZ, et al. Selective Chk1 inhibitors differentially sensitize p53-deficient cancer cells to cancer therapeutics. Int J Cancer 2006;119:2784–94.
32. Liu Q, Guntuku S, Cui XS, et al. Chk1 is an essential kinase that is regulated by Atr and required for the G(2)/M DNA damage checkpoint. Genes Dev 2000;14:1448–59.
33. Rodriguez R, Meuth M. Chk1 and p21 cooperate to prevent apoptosis during DNA replication fork stress. Mol Biol Cell 2006;17:402–12.
34. Andreyev AY, Kushnareva YE, Starkov AA. Mitochondrial metabolism of reactive oxygen species. Biochemistry (Mosc) 2005;70:200–14.
35. Kim CJ, Lee JH, Song JW, et al. Chk1 frameshift mutation in sporadic and hereditary non-polyposis colorectal cancers with microsatellite instability. Eur J Surg Oncol 2007;33:580–5.
36. Verlinden L, Vanden Bempt I, Eelen G, et al. The E2F-regulated gene Chk1 is highly expressed in triple-negative estrogen receptor/progesterone receptor/HER-2 breast carcinomas. Cancer Res 2007;67:6574–81.
37. Collins I, Garrett MD. Targeting the cell division cycle in cancer: CDK and cell cycle checkpoint kinase inhibitors. Curr Opin Pharmacol 2005;5:366–73.
38. Schneider-Stock R, Boltze C, Peters B, et al. Selective loss of codon 72 proline p53 and frequent mutational inactivation of the retained arginine allele in colorectal cancer. Neoplasia 2004;6:529–35.